or

$$\rho_{o1} = -f_2 m(\rho_{1,o} - \rho_{2,o}) \qquad \text{(A9a)}$$

$$\rho_{o2} = f_1 m(\rho_{1,o} - \rho_{2,o}) \qquad \text{(A9b)}$$

Introducing this into eq A7, we finally get

$$\alpha = -f_1 f_2(\rho_{1,o} - \rho_{2,o})[R_1^2 - R_2^2 - (f_1 - f_2)d^2] \quad \text{(A10)}$$

$$\beta = f_1^2 f_2^2(\rho_{1,o} - \rho_{2,o})^2 d^2$$

This is in disagreement with the corresponding formula for β by Koch and Stuhrmann (1978), which also lacks the volume fractions.

In the case of an exactly symmetrical exchange of particles 1 and 2, i.e., $\rho_{1,o} = \rho_{2,o}$ and $\rho_{2,o} = \rho_{1,o}$, β remains unchanged and α changes its sign, but not it values, leading to Stuhrmann plots (R^2 vs $1/\bar{\rho}$) which are symmetrical with respect to the $1/\bar{\rho}$ axis. If, however, this symmetry is not fulfilled, e.g., because the level of deuteration of constituent 1 is not the same as that of constituent 2, α and β are different for the pairs H_1D_2 and D_1H_2.

If the constituents are of unequal size, the Stuhrmann plot of one of these pairs can be shifted sufficiently far away from the origin of $1/\bar{\rho}$ that the curvature of the parabola cannot be observed due to the errors of the radius of gyration determinations at low contrasts, i.e., large $1/\bar{\rho}$ values (Figure 7). It is important to note that inhomogeneity of one of the constituents is *not* required for explaining this fact (although it might be easier to use this explanation for chemical reasons).

REFERENCES

Cotton, J. P., & Benoit, H. (1975) *J. Phys. 36*, 905–910.
Damaschun, G., Fichtner, P., Pürschel, H. V., & Reich, J. G. (1968) *Acta Biol. Med. Ger. 21*, 309–316.
Koch, M. H. J., & Stuhrmann, H. B. (1979) *Methods Enzymol. 59*, 670–706.
Moore, P. B. (1981) *J. Appl. Crystallogr. 14*, 237–240.
Stuhrmann, H. B., Tardieu, A., Mateu, L., Sardet, C., Luzzati, V., Aggerbeck, L., & Scanu, A. M. (1975) *Proc. Natl. Acad. Sci. U.S.A. 72*, 2270–2273.
Stuhrmann, H. B., Koch, M. H. J., Parfait, R., Haas, J., Ibel, K., & Crichton, R. R. (1978) *J. Mol. Biol. 119*, 203–212.
Witz, J. (1983) *Acta Crystallogr. A39*, 706–711.

On the Mechanism of Transbilayer Transport of Phosphatidylglycerol in Response to Transmembrane pH Gradients[†]

T. E. Redelmeier,[‡] M. J. Hope,[‡,§] and P. R. Cullis[*,‡,§]

Department of Biochemistry, The University of British Columbia, Vancouver, British Columbia, Canada V6T 1W5, and The Canadian Liposome Company Ltd., Suite 308, 267 Esplanade, North Vancouver, Canada V7M 1A5

Received July 24, 1989; Revised Manuscript Received November 8, 1989

ABSTRACT: Previous work [Hope et al. (1989) *Biochemistry 28*, 4181–4187] has shown that asymmetric transmembrane distributions of phosphatidylglycerol (PG) in PG–phosphatidylcholine (PC) large unilamellar vesicles can be induced in response to transbilayer pH gradients (ΔpH). Here the mechanism of PG transport has been investigated. It is shown that PG movement in response to ΔpH is consistent with permeation of the uncharged (protonated) form and that the half-time for transbilayer movement of the uncharged form can be on the order of seconds at 45 °C. This can result in rapid pH-dependent transmembrane redistributions of PG. The rate constant for transbilayer movement exhibits a large activation energy (31 kcal/mol) consistent with transport of neutral dehydrated PG where dehydration of the (protonated) phosphate presents the largest barrier to transmembrane diffusion. It is shown that acyl chain saturation, chain length, and the presence of cholesterol modulate the rate constants for PG transport in a manner similar to that observed for small nonelectrolytes.

P hospholipids in biological membranes frequently exhibit asymmetric transbilayer distributions. This has been shown for the erythrocyte plasma membrane (Op den Kamp, 1979), the platelet plasma membrane (Chap et al., 1977), the rat liver endoplasmic reticulum (Higgins & Pigott, 1982; Sleight & Pagano, 1985), the Golgi complex (van Meer et al., 1987), and the inner mitochondrial membrane (Krebs et al., 1978). Two general findings have been made. First, in the plasma membrane of the erythrocyte, lymphocyte, or platelet, the amino-containing phospholipids phosphatidylserine and phosphatidylethanolamine are primarily located in the inner (cytoplasmic) monolayer (IM)[1] whereas the choline-containing lipids phosphatidylcholine (PC) and sphingomyelin are located in the outer monolayer (OM). Second, the transbilayer

[1] Abbreviations: BSA, bovine serum albumin; Chol, cholesterol; DOPC, dioleoylphosphatidylcholine; DOPG, dioleoylphosphatidylglycerol; DPoPC, dipalmitoleoylphosphatidylcholine; DPPC, dipalmitoylphosphatidylcholine; EPC, egg phosphatidylcholine; EPG, egg phosphatidylglycerol; EPPS, *N*-(2-hydroxyethyl)piperazine-*N'*-3-propanesulfonic acid; HEPES, *N*-(2-hydroxyethyl)piperazine-*N'*-2-ethanesulfonic acid; IM, inner monolayer; LPC, lysophosphatidylcholine; LUVs, large unilamellar vesicles; MES, 2-(*N*-morpholino)ethanesulfonic acid; MOPG, monooleoylphosphatidylglycerol; OM, outer monolayer; PA, phosphatidic acid; PG, phoshatidylglycerol; PIPES, piperazine-*N*,-*N'*-bis(2-ethanesulfonic acid); PS, phosphatidylserine; SA, stearylamine.

movement of phospholipids is slow, with half-times ranging from hours for the erythrocyte plasma membrane to times on the order of days for model membrane (protein-free) systems (Op den Kamp, 1979).

Recent work from this laboratory has shown that lipids which exhibit simple weak acid or weak base characteristics rapidly redistribute across large unilamellar vesicle (LUV) membranes in response to transmembrane pH gradients. This includes stearic acid, stearylamine, and sphingosine (Hope & Cullis, 1987) as well as certain phospholipids which have weak acid characteristics, such as phosphatidylglycerol (PG) and phosphatidic acid (PA) (Hope et al., 1989). In this work, we examine in detail for PG the mechanism whereby this redistribution process occurs. The results indicate that transbilayer movement of PG occurs via permeation of the uncharged (protonated), dehydrated form which can exhibit half-times for transbilayer transport on the order of seconds.

MATERIALS AND METHODS

Materials. Phospholipids were purchased from Avanti Polar Lipids and used without further purification. Cholesterol was purchased from Sigma Chemical Co. Radiochemicals were purchased from New England Nuclear. Pyranine was purchased from Molecular Probes. All other buffers and chemicals were of analytical grade.

Preparation of Lysophosphatidylglycerol. Monooleoylphosphatidylglycerol (MOPG) was prepared by the following procedure. Dioleoylphosphatidylglycerol (DOPG) (1 g) was dissolved to clarity in 60 mL of ether containing 0.6 mL of water. Phospholipase A_2 (1000 units of *Croatalus adamenteus*, Sigma) dissolved in 2.5 mL of 200 mM sodium borate (pH 7.4) was added to the ether solution, and the mixture was agitated for 1 h at 30 °C. The extent of the reaction was monitored by TLC, and upon completion, the precipitate was recovered by centrifugation. The precipitate was resuspended in a minimum volume of ethanol, and further precipitations (by the addition of 200 mL of ice-cold ether) were carried out until the MOPG was greater than 95% pure as judged by TLC.

Preparation of LUVs. Lipids were mixed in chloroform which was subsequently removed under a stream of nitrogen followed by exposure to high vacuum for at least 1 h. Multilamellar vesicles were prepared by vortexing the resulting lipid film in the presence of the appropriate buffer (50 mg/mL, w/v) for 15 min. The lipid dispersion was then frozen and thawed 5 times to obtain equilibrium transmembrane solute distributions (Mayer et al., 1985). The resulting frozen and thawed vesicles were then repeatedly (10X) extruded through two (stacked) polycarbonate filters of 100-nm pore size using an extrusion device (Lipex Biomembranes, Vancouver, B.C.). The resulting large unilamellar vesicle (LUVs) exhibit trapped volumes of 1.5 μL/μmol of phospholipid and an average diameter of 90 nm (Hope et al., 1985).

Induction of Transbilayer Transport of PG. Vesicles prepared in 300 mM NaEPPS (pH 9.0) were passed down a G-50 gel filtration column equilibrated in 150 nM Na_2SO_4 (or 200 mM where indicated) and 1 mM EPPS (pH 9.0). Aliquots (50 μL) of the eluant (10–20 mg/mL phospholipid) were then incubated at the appropriate temperature for 5 min. Typically, transport (import) of PG was initiated by adding an aliquot (80 μL) of a buffer consisting of 100 mM sodium sulfate/100 mM sodium citrate (pH 4.0) (45 °C) to establish the transmembrane pH gradient. Lipid redistribution was stopped by an addition of 0.7 mL of ice-cold buffer consisting of 100 mM sodium acetate/100 mM citrate (pH 6.0). These conditions inhibit subsequent transport of PG as the rate of transport is

markedly reduced at low temperature (see Results), the acetic acid acts to dissipate the pH gradient (inside basic), and the higher external pH reduces the concentration of the neutral (membrane permeable) form of PG (see Results). The samples were then held at 4 °C until analyzed for PG asymmetry. The extent of PG asymmetry was stable at 4 °C for at least 24 h (data not shown).

Detection of PG Transbilayer Asymmetry. Transmembrane asymmetry of PG was determined by the periodate oxidation assay previously described (Lentz et al., 1980; Hope et al., 1989). Analysis of PG asymmetry in vesicles was performed at 25 °C except for vesicles containing DPPC which were incubated at 45 °C (above the lipid-phase transition temperature). Oxidation of the PG present in the external monolayer was initiated by the addition of 100 μL of freshly prepared 100 mM sodium periodate to samples prepared as described above. The oxidation was quenched after 12 min by the addition of 100 μL of 1 M sodium arsenite in 0.5 M H_2SO_4. Formaldehyde produced by the oxidation of the PG was detected by the Hantzsh reaction (Nash, 1953). Control experiments demonstrated that a 12-min oxidation of the PG in vesicles exhibiting no pH gradient resulted in oxidation of 50% of the PG present in the sample. Control experiments also demonstrated that 3-phosphoglycerol entrapped in EPC LUVs has not oxidized under these standard conditions, indicating that the periodate only has access to the outer monolayer (OM) PG.

Detection of Transmembrane pH Gradients. EPC/EPG (9:1 mol/mol) LUVs were prepared in 300 mM NaEPPS (pH 9.0) as described above except that the fluorescent pH indicator pyranine (1 mM) (Clement & Gould, 1981) was included in the buffer. The external buffer was then exchanged for 150 mM Na_2SO_4/1 mM EPPS (pH 9.0) using gel filtration as described above. Control experiments demonstrated that when pyranine was added to preformed vesicles it was removed below detection levels during gel filtration. Thus, the remaining pyranine associated with the vesicles is entrapped. The fluorescent response of the entrapped pyranine to changes in pH was then calibrated. Vesicles were diluted (to approximately 1 mM phospholipid) in 150 mM Na_2SO_4, 20 mM EPPS, 20 mM HEPES, 20 mM PIPES, and 20 mM MES which had been adjusted to a range of pH values (pH 5.0–9.0) with NaOH. Nigericin (final concentration of 100 nM) and gramicidin (final concentration of 10 μg/mL) were added to the vesicle solution to facilitate equilibration of transmembrane proton gradients. A standard curve was developed by calibrating the fluorescent response of the entrapped pyranine to changes in the external pH in the presence of proton ionophores. The internal pH of vesicles exhibiting a transmembrane pH gradient (pH 9.0 inside/pH 4.0 outside) was monitored over time by following the fluorescence response of the entrapped pyranine and converting it to an internal pH by comparison with the calibration curve.

Transmembrane Distribution of Lysophosphatidylcholine. EPC/EPG (9:1 mol/mol) LUVs (10 mg of phospholipid/mL) were prepared as described above except that trace amounts of [³H]DPPC (0.1 μCi/mL) and [¹⁴C]LPC (0.1 μCi/mL) were included with the lipid before solvent evaporation. Transmembrane pH gradients (pH 9.0 inside/pH 4.0 outside) were established as described above, and the sample (0.1 mL) was incubated at 45 °C for the indicated time period. The incubation was stopped by the addition of 0.4 mL of cold 100 mM sodium acetate/100 mM sodium citrate (pH 6.0) containing 50 mg/mL fatty acid free bovine serum albumin (BSA, Sigma Chemical Co). BSA was included in this buffer in order

to remove the LPC from the OM of the LUVs. The vesicles were then separated from BSA employing a Sepharose 4-B gel filtration column. Control experiments demonstrated that in the absence of BSA all of the [^{14}C]LPC eluted with the liposomes. Recovery of liposomes from the column was typically greater than 95%. Fractions of the eluant were counted on a Packard 2000CA liquid scintillation counter to determine the amount of LPC associated with the IM of the vesicles.

Kinetic Analysis of Phosphatidylglycerol Transport. Weak acids are normally transported across lipid bilayers as the protonated (neutral) species [for example, see Gutnecht and Walter (1981a)]. Consequently, the net inward flux (J_{net}) of PG is expected to be a function of the concentration gradient of the neutral species, the membrane area, and the rate constant for translocation of the neutral form according to

$$J_{net} = (1/A_m)[dN(A)_o^{tot}/dt] = -K([AH]_o - [AH]_i) \quad (1)$$

where $N(A)_o^{tot}$ is the total number of PG molecules in the exterior monolayer, [AH] is the (surface) concentration of the neutral form of the acid, K is the rate constant for transport of the neutral form, A_m is the area of the membrane, and the subscripts o and i refer to the OM and IM, respectively. Writing the weak acid dissociation constant as $K_a = [A^-][H^+]/[AH]$ and assuming that only the neutral (AH) form is membrane-permeable, it is straightforward to show that

$$(1/A_m)[dN(A)_o^{tot}/dt] = d[A(t)]_o^{tot}/dt =$$
$$(1 + K_a/[H^+]_o)d[AH]_o/dt \quad (2)$$

where $[A(t)]_o^{tot}$ is the total concentration of PG, both charged and uncharged, in the outer monolayer. Under the conditions that $K_a \gg [H^+]_o$, $[H^+]_i \ll [H^+]_o$, it follows that

$$[A(t)]_o^{tot} = [A(0)]_o^{tot}e^{-kt} + [A(eq)]_o^{tot} \quad (3)$$

where $k = [H^+]_o K/K_a$ and $[A(eq)]_o^{tot}$ is the equilibrium value of $[A]_o^{tot}$. Thus

$$\ln[([A(t)]_o^{tot} - [A(eq)]_o^{tot})/[A(o)]_o^{tot}] = -kt \quad (4)$$

Consequently, a plot of ln $[([A(t)]_o^{tot} - [A(eq)]_o^{tot})/[A(0)]_o^{tot}]$ vs time should yield a straight line with slope k which has units of t^{-1}. The half-time for transbilayer movement is then given by $t_{1/2} = 0.693k^{-1}$. It should also be noted that a plot of log k vs log [H$^+$]$_o$ should yield a straight line with a slope of unity if k is directly proportional to [H$^+$]$_o$.

Rate parameters were determined by applying a nonlinear least-square analysis to the data using a commercially available plotting program (Sigma-Plot, Jandel Scientific, 1986). The best fit to the data was obtained by employing k and $[A(eq)]_o^{tot}$ as variables.

RESULTS

Kinetic Analysis of Transport of PG across LUVs. Initial experiments were designed to demonstrate ΔpH-induced asymmetry for EPG and to investigate the applicability of the kinetic analysis developed under Materials and Methods. In this regard, the results of Figure 1A illustrate that the presence of a pH gradient (inside basic) results in the movement of PG into the inner monolayer (IM) of EPC/EPG (9:1) LUVs held at 45 °C. Approximately 50% of the PG in the outer monolayer (OM) is transported to the IM within 50 min. This corresponds to approximately 5% net transport of the total OM lipid to the IM under conditions where one would not expect transport of IM lipid (EPC) to the OM. The movement of PG demonstrated in Figure 1A is slower than that observed for weak acids such as stearic acid where greater than 95% asymmetry is observed after a 5-min incubation at 25 °C
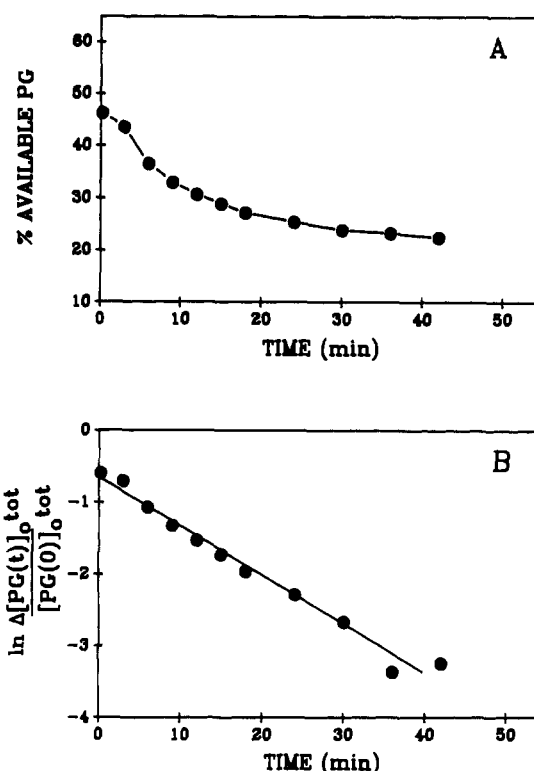

FIGURE 1: Influence of a pH gradient (interior basic) on the transbilayer distributions of PG in LUVs. P and A illustrates the time course of PG transport from the outer monolayer to the inner monolayer of LUVs in response to the pH gradient. EPC/EPG (9:1 mol/mol) LUVs were prepared in 300 mM EPPS (pH 9.0), and the external buffer was exchanged for 150 mM sodium sulfate/1 mM EPPS (pH 9.0). The transport at 45 °C was initiated by the addition of an aliquot of 100 mM sodium citrate (pH 4.0), and transport was stopped by adding an aliquot of cold 100 mM sodium citrate/acetate (pH 6.0). The PG asymmetry was determined by employing the periodate assay as described under Materials and Methods. Panel B illustrates the best fit to this data employing the first-order kinetic analysis described under Materials and Methods. Note that Δ[PG-(t)]$_o^{tot}$ = [PG(t)]$_o$ - [PG(eq)]$_o$.

(Hope & Cullis, 1987). It is, however, considerably more rapid than phospholipid transport generally observed in model membranes (Op den Kamp, 1979).

The presence of a transmembrane pH gradient is expected to result in transmembrane gradients of weak acids according to [A]$_i$/[A]$_o$ = [H$^+$]$_o$/[H$^+$]$_i$. Thus, a gradient of greater than 2 units should result in a PG transmembrane gradient of greater than 100-fold. In previous work (Hope & Cullis, 1987), we have shown that greater than 95% of stearic acid is sequestered into LUVs in response to a transmembrane pH gradient of greater than 2 units (inside basic). However, the data of Figure 1A indicate that the PG transport reaches an equilibrium at an inside:outside ratio of 3:1. Thus, the degree of asymmetry is considerably less than that expected for the transbilayer distribution of a membrane-bound weak acid (>100:1) in response to a bulk pH gradient of 2 units or more. As a result, a fit of the data of Figure 1A by the kinetic analysis indicated under Materials and Methods using an equilibrium value ([A(eq)]$_o^{tot}$) obtained assuming an inside:outside ratio for PG of 100:1 could not be achieved. However, as illustrated in Figure 1B, a good fit can be obtained if [A(eq)]$_o^{tot}$ is estimated as the amount of exterior PG remaining at 5 half-lives (60 min). The rate constant for transport (k) can be calculated to be 0.06 min^{-1} ($t_{1/2}$ = 12 min).

Stability of the Basic pH Gradient during PG Transport. It is important to demonstrate that the pH gradient which
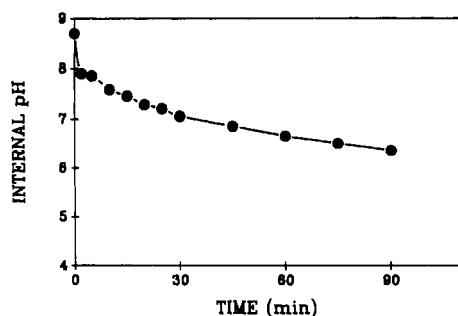
FIGURE 2: Measurement of the pH gradient (basic interior) maintained during PG import by entrapped pyranine. EPC/EPG (9:1 mol/mol) LUVs were prepared in 1 mM pyranine/300 mM NaEPPS (pH 9.0), and the external buffer was exchanged for 150 mM sodium sulfate/1 mM NaEPPS (pH 9.0). A standard curve was prepared as described under Materials and Methods relating the external pH (in the presence of ionophores) with the fluorescence response of the entrapped pyranine. The incubation at 45 °C was initiated by adding an aliquot of 100 mM sodium citrate (pH 4.0), and the internal pH was monitored over the indicated time period.

drives the asymmetry illustrated in Figure 1 does not dissipate over the time course of the experiment. An assay based on the pH dependence of the membrane-impermeable fluorescent dye pyranine was used to detect the transmembrane pH gradient (inside basic) [Materials and Methods; see also Elamri and Blume) (1981)]. The results of Figure 2 demonstrate the time dependence of the internal pH after a pH gradient (pH 9.0 inside/pH 4.0 outside) has been established. Over a 1-h time course at 45 °C, the internal pH decreased from 9 to 6.5. The reduction is biphasic with a rapid fall occurring during the first 2 min and a slower reduction occurring over the rest of the time course. The important point is that the equilibrium PG distribution observed at 30 min does not appear to be limited by dissipation of the transmembrane pH gradient.

Transport of Lysophosphatidylcholine. It is of interest to examine whether the inward ("flip") movement of PG drives the outward ("flop") movement of another lipid. Since the extent of transport can be expected to be very low under these conditions, it was not possible to measure transport of EPC or an analogue since an adequately sensitive assay for monitoring transbilayer distributions of EPC was not available. However, asymmetry of radiolabeled lysophosphatidylcholine (LPC) can be readily monitored by comparing the amount of LPC which can be extracted from LUVs by BSA to that which cannot be removed. This is shown by the results of Figure 3A, which illustrates the elution profile of EPC/EPG (9:1 mol/mol) LUVs containing radiolabeled LPC employing a CL-2B gel filtration column. In the absence of BSA in the external buffer, radiolabeled LPC coelutes with the liposomes as monitored by radiolabeled DPPC (data not shown). However, inclusion of BSA in the external buffer causes 57% of the [14C]LPC to be retained by the column without influencing the elution profile of the EPC vesicles. The elution behavior of the retained fraction coincides with that of BSA. The amount of LPC that can be extracted from the vesicles was found to be insensitive to increases in the amount of BSA present in the external buffer, indicating that all of the LPC has been removed from the OM of the vesicles under these conditions. This indicates that the transbilayer distribution of LPC in these LUVs is 57% in the OM and 43% in the IM. The results of Figure 3B demonstrate that the amount of LPC which can be extracted by BSA from EPC/EPG (9:1 mol/mol) LUVs is not altered by the movement of PG from the OM to the IM. This provides indirect evidence that exterior PG does not "flip" into the IM concurrently with the "flop" of another lipid out of the IM.
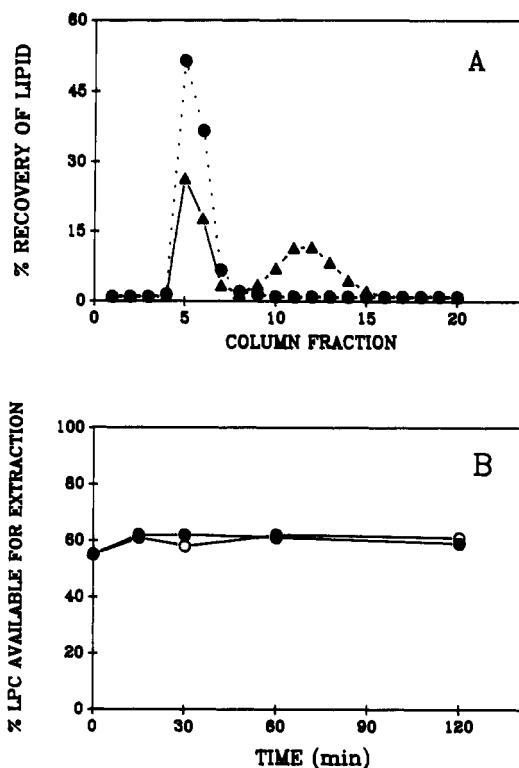

FIGURE 3: Influence of PG transport on the transbilayer distribution of LPC. EPC/EPG (9:1 mol/mol) LUVs containing trace amounts of [3H]DPPC and [14C]LPC were prepared in 300 mM NaEPPS (pH 9.0), and the external buffer was exchanged for 150 mM sodium sulfate/1 mM NaEPPS (pH 9.0). The transport at 45 °C was initiated by adding an aliquot of 100 mM sodium citrate (pH 4.0) and was stopped by adding cold 100 mM sodium acetate/100 mM citrate (pH 6.0) containing 50 mg/mL fatty acid free BSA. The asymmetry of LPC was determined as described under Materials and Methods. Panel A indicates the elution profile of LPC (▲) and the LUVs (●) employing a Sepharose 4-B gel filtration column used to separate LUVs from the included BSA. Panel B indicates the amount of LPC in the outer monolayer for vesicles exhibiting PG asymmetry (●) and in vesicles which do not exhibit PG asymmetry (O).

Temperature Dependence of PG Transport. Factors which influence the rate of PG translocation were examined to clarify the mechanism of transport. The results of Figure 4A demonstrate the temperature dependence, which is remarkable for a simple diffusion process as the rate increases 3-fold for every 7 °C rise in temperature. It is unlikely that the temperature dependence is due to an influence of temperature on the external pH as the pK_a^2 of citrate changes less than 0.04 unit for a 30 °C change in temperature (*Lange Handbook of Chemistry*, 1979). Figure 4B shows an Arrhenius plot of the data of Figure 4A from which an activation energy of 31 kcal mol^{-1} may be calculated. This compares favorably with that reported by Homan and Pownall (1988) (34 kcal mol^{-1}) for the transbilayer transport of a short-chain fluorescent analogue of PG in SUVs.

pH Dependence of PG Transport. Weak acids and bases are generally thought to permeate across membranes as the neutral species (Gutnecht & Walter, 1981b). However, there have been reports that weak bases can cross model membranes as the charged species (McLaughlin, 1975). Furthermore, it has been suggested that fatty acids can act as proton ionophores in model membrane systems, which suggests that they can move across the membrane in both the charged and also the neutral form (Gutnecht & Walter, 1981a). The pH dependence of the PG transport should distinguish between the two mechanisms of transport. As indicated under Materials and Methods, the rate of transport should be influenced by
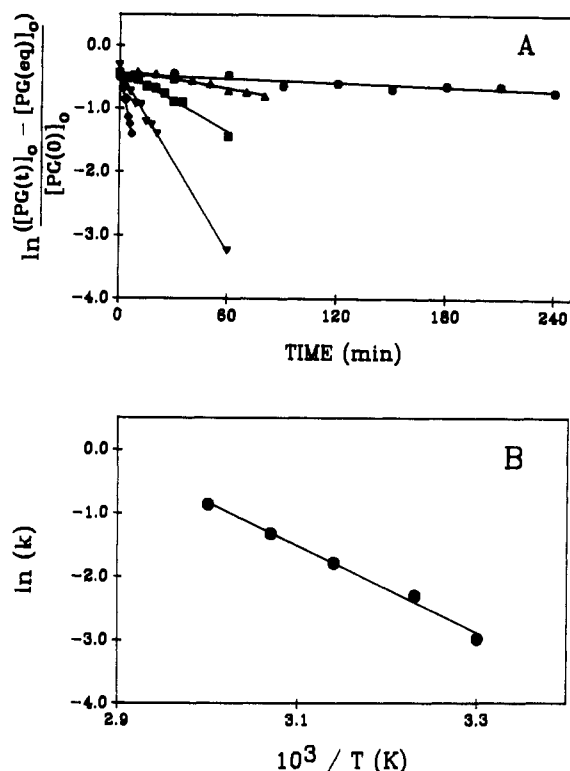
FIGURE 4: Influence of temperature on PG transport. EPC/EPG (9:1 mol/mol) LUVs were prepared in 300 mM NaEPPS (pH 9.0), and the external buffer was exchanged for 150 mM sodium sulfate/1 mM NaEPPS (pH 9.0). The transport was initiated at a given temperature by adding an aliquot of 100 mM sodium citrate (pH 4.5) preequilibrated at the indicated temperature, and the transport was stopped by adding cold 100 mM sodium acetate/100 mM citrate (pH 6.0). The PG asymmetry was determined as described under Materials and Methods. Transport was followed at (●) 30, (▲) 37, (■) 45, (▼) 52, and (♦) 59 °C and treated by the kinetic analysis (see Materials and Methods) as depicted in (A) to extract the rate constant k. An Arrhenius plot of the rate constants is shown (B).

Table I: Lipid Factors Which Influence the Half-Time for PG Transbilayer Transport[a]

lipid composition	temp (°C)	$t_{1/2}$ (min)
DPPC/EPG 9:1	50	13
DPoPC/EPG 9:1	50	3.6
DOPC/EPG 9:1	50	7.1
DOPC/DOPG 9:1	45	13.5
DOPC/MOPC/DOPG 8:1:1	45	10.6
DOPC/MOPG 9:1	45	11.2
EPC/EPG 9:1	45	12.4
EPC/Chol/EPG 8:1:1	45	11.7
EPC/Chol/EPG 7:2:1	45	14.4
EPC/Chol/EPG 6:3:1	45	36.3
EPC/Chol/EPG 5:4:1	45	63.0
EPC/EPG 9:1	45	15.1
EPC/PS/EPG 8:1:1	45	12.2
EPC/PS/EPG 7:2:1	45	9.9
EPC/EPG 9.5:0.5	45	12.4
EPC/EPG 9:1	45	10.7
EPC/EPG 8:2	45	8.9
EPC/EPG 7:3	45	8.0

[a] LUVs were prepared in 300 mM NaEPPS (pH 9.0), and the external buffer was exchanged for 150 mM sodium sulfate/1 mM NaEPPS (pH 9.0). The transport at the indicated temperature was initiated by adding an aliquot of 100 mM sodium citrate (pH 4.0) and was stopped by adding cold 100 mM sodium acetate/100 mM citrate (pH 6.0). The PG asymmetry was determined and analyzed as described under Materials and Methods. The data are the mean of two independent experiments in which the rate constant was determined with no less than eight time points performed in duplicate.

the pH of the external buffer if PG is transported as the neutral species since the rate constant (k) is then proportional to $[H^+]_o$.
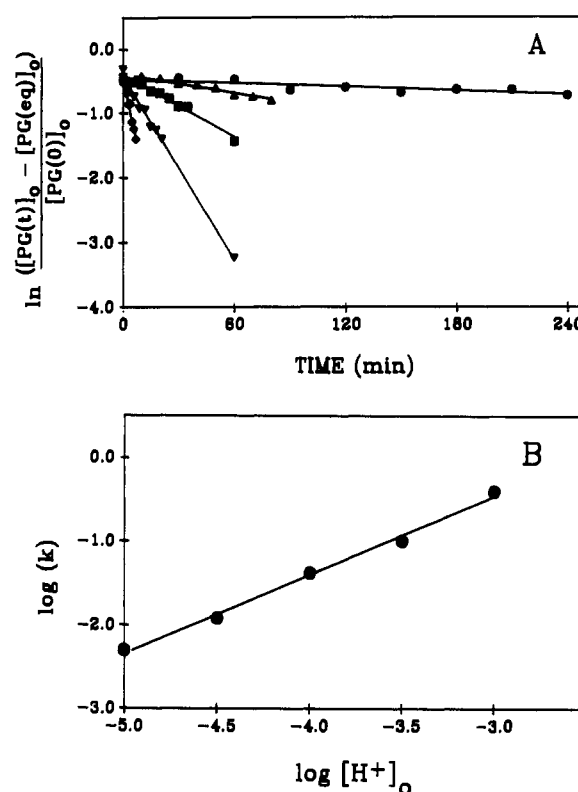

FIGURE 5: Influence of the external pH on PG transport at 45 °C. EPC/EPG (9:1 mol/mol) LUVs were prepared in 300 mM NaEPPS (pH 9.0), and the external buffer was exchanged for 200 mM sodium sulfate/1 mM NaEPPS (pH 9.0). The transport was initiated by adding an aliquot of 100 mM sodium citrate which had been adjusted to the indicated pH. The transport was stopped by adding cold 100 mM sodium acetate/100 mM citrate (pH 6.0). The PG asymmetry was determined as described under Materials and Methods. Transport was followed at pH 5.0 (●), 4.5 (▲), 4.0 (■), 3.5 (▼), and 3.0 (♦) and treated by the kinetic analysis described under Materials and Methods (A). A plot of log k vs the external proton concentration is shown in (B), from which a slope of 0.95 ± 0.5 can be calculated.

However, transport of the charged species would not be expected to be influenced by the pH of the external medium. The results of Figure 5A demonstrate that the rate of transport is markedly sensitive to the pH of the external medium. For example, decreasing the external pH from 4 to 3 increases the rate of transport 10-fold, as expected for transport via the neutral species. A linear relationship between the rate constant for transport and the exterior H^+ ion concentration is indicated by the plot of the log of the rate constants (k) derived from Figure 5A vs log $[H^+]_o$ which exhibits a slope of 0.95 ± 0.050 (Figure 5B). As indicated under Materials and Methods, this is consistent with transport of the neutral (protonated) species.

Influence of Lipid Composition on PG Transport. It is well-known that the permeability of lipid bilayers to neutral solutes is sensitive to lipid composition. For example, increased saturation, chain length, or the inclusion of cholesterol can dramatically decrease permeability rates. If PG is transported in the neutral form, similar effects should be observed. In this regard, Table I summarizes the influence of a variety of lipid compositions on ΔpH-induced PG transport across LUV membranes. Comparison of the transport rates for EPG in dipalmitoylphosphatidylcholine (DPPC) vesicles with those for vesicles composed of an unsaturated lipid (dipalmitoleoylphosphatidylcholine, DPoPC) indicates the sensitivity of PG transport to lipid saturation, where EPG is transported at approximately half the rate in a DPPC matrix as compared to the DPoPC system. In addition, the movement of EPG is sensitive to the length of the acyl chain of the host matrix,

decreasing with increasing acyl chain length. Thus, the import of EPG in vesicles composed of DOPC was approximately 50% slower than in the DPoPC system.

The results of Table I also demonstrate that transbilayer transport of MOPG in DOPC (9:1 mol/mol) LUVs is similar to that of DOPG in LUVs composed of a DOPC/MOPC/DOPC mixture (8:1:1 mol/mol). This similarity indicates that the primary energetic barrier to PG transport is the polar headgroup. The results of Table I also demonstrate that cholesterol strongly influences the rate of PG translocation. However, the dependence in not linear. At concentrations below 20 mol %, PG translocation is reduced by a maximum of only 16% whereas at higher cholesterol contents transport is markedly slower.

The transport of PG in response to pH gradients would be expected to be sensitive to the surface charge of the vesicles, due to the influence of surface charge on the interfacial pH. The results of Table I indicate that the presence of 20 mol % PS in the EPC matrix slightly increased the rate of PG transport. PS is not transported under these conditions (results not shown). This increase rate is consistent with a slight increase in the negative surface charge of the vesicles which in turn would lead to a decrease in the interfacial pH and a correspondingly greater proportion of PG in the neutral form. The observation that increasing the concentration of PG in the vesicles from 5 to 30 mol % causes an increased rate of transport (Table I) is also consistent with this hypothesis.

Factors Which Influence the Extent of PG Asymmetry. As previously noted, the equilibrium value for transmembrane PG asymmetry is less than expected for the transmembrane distribution of a weak acid in response to a pH gradient of greater than 2 units. Two factors which could influence the maximum amount of PG transported include packing constraints in the monolayer to which PG is transported and surface charge effects. There are three lines of evidence that packing constraints do not play a direct role in limiting PG transport. First, if such packing constraints are limiting the amount of PG transported in the systems containing 5 mol % PG, then no further increase in PG transport should be observed at higher PG contents. However, as shown in Table II, increasing the PG content from 5 to 30 mol % results in an increase in the amount of PG transported by a factor of 2.9. A second point is that inclusion of cholesterol, which is well-known to increase lipid packing and order in the hydrocarbon (Davis, 1986), would be expected to influence (and possibly reduce) the maximum PG asymmetry achievable if packing constraints were limiting. As indicated in Table II, however, increasing the cholesterol content to 40 mol % had little effect on the maximum extent of asymmetry. A third point is that if hydrocarbon packing is limiting, greater asymmetry should be observed for lyso-PG as compared to PG. As again indicated in Table II, however, MOPG was transported to the same extent as DOPG.

With regard to surface charge effects it may be suggested that accumulation of PG into the inner monolayer results in surface charges sufficient to reduce the interfacial pH (as compared to the interior bulk phase pH) to the extent that further transport is inhibited. This is unlikely, however, as even if all the PG in the 10 mol % system was present on the inner monolayer, this would only correspond to a surface potential of 40 mV at the internal buffer concentrations employed here (300 mM NaEPPS). This would reduce the interfacial pH by only 0.7 unit as compared to the bulk phase. It may also be noted that inclusion of 5 mM Mn^{2+} in the internal or external buffers did not affect the observed asym-

Table II: Lipid Factors Which Influence the Extent of PG Transport[a]

lipid composition	temp (°C)	PG transported (% of OM PG)
EPC/EPG 9.5:0.5	45	54
EPC/EPG 9:1	45	44
EPC/EPG 8:2	45	27
EPC/EPG 7:3	45	26
EPC/EPG 9:1	45	50
EPC/PS/EPG 8:1:1	45	48
EPC/PS/EPG 7:2:1	45	51
EPC/PA/EPG 8:1:1	45	32
DOPC/DOPG 9:1	45	60
DOPC/MOPG 9:1	45	60
DOPC/MOPC/DOPG 8:1:1	45	66
EPC/EPG 9:1	45	58
EPC/Chol/EPG 8:1:1	60	58
EPC/Chol/EPG 7:2:1	60	60
EPC/Chol/EPG 6:3:1	60	66
EPC/Chol/EPG 5:4:1	60	60

[a] LUVs were prepared in 300 mM NaEPPS (pH 9.0), and the external buffer was exchanged for 200 mM sodium sulfate/1 mM NaEPPS (pH 9.0). The transport was initiated by adding an aliquot of 100 mM sodium citrate/sodium sulfate (pH 4.0), and the transport was stopped by adding cold 100 mM sodium acetate/100 mM sodium citrate (pH 6.0) at 60 or 30 min, respectively. The PG asymmetry was determined as described under Materials and Methods.

metry (results not shown). Similarly, inclusion of up to 20 mol % PS (which is not transported) did not influence the extent of PG asymmetry at equilibrium. However, it is interesting to note that in the presence of 10 mol % PA (Table II), a lipid that will also accumulate at the IM under these conditions (Hope et al., 1989), PG asymmetry is reduced.

DISCUSSION

The results presented here provide new insight into the mechanism of transport of phosphatidylglycerol in reponse to transmembrane pH gradient, factors which modulate such transport, and demonstrate the resulting redistribution can be relatively rapid. With regard to mechanism, the data presented are consistent with a first-order process involving permeation of the uncharged (protonated) form of PG. This is indicated in part by an ability to fit the data to the first-order formalism described under Materials and Methods. More direct evidence is given by the proportionality between the rate constant k and the exterior proton concentration, which strongly supports permeation of the neutral form. This behavior is consistent with the generally accepted view that weak acids and bases permeate across membranes in the neutral form [see, for example, Gutnecht and Walter (1981b)]. A consequence is that the transbilayer movement of PG in these systems proceeds by simple monomer diffusion and does not involve a "flip-flop" process such as suggested by Bretscher (1971). This conclusion is supported by the lack of any outward movement of lyso-PC during PG accumulation.

Interestng features of the ΔpH-induced migration of PG concern the rapid nature of the permeation process and the sensitivity to experimental variables. As indicated under Results, the rate constant k for the transbilayer movement of PG at 45 °C, pH_o = 4.0, is approximately 6×10^{-2} min^{-1}. From the relation $k = [H^+]_o K/K_a$ (see Materials and Methods), and assuming that the pK_a of the PG phosphate is 2 (Watts et al., 1978), this corresponds to a rate constant for transport of the neutral form of K = 6 min^{-1}, or a half-time for transbilayer movement of approximately 7 s. This is considerably faster than previously observed for phospholipids in model (Op den Kamp, 1979) and biological (Seigneuret & Devaux, 1984) systems, where half-times in the range of hours to days are commonly observed. On the other hand, it is a

rate consistent with that observed for the neutral diacylglycerol molecule (Ganong & Bell, 1984). It therefore follows that conditions which lead to generation of a small fraction of neutral species of a given phospholipid may be expected to give rise to greatly enhanced transbilayer migration.

The high activation energy observed for PG translocation has implications for the form of the membrane-permeable intermediate. Briefly, it has been previously observed that a strong correlation exists between the activation energy for transbilayer transport of a variety of short-chain alcohols and the number of hydrogen bonds that could be formed (de Gier et al., 1970; Cohen, 1975), consistent with transport of a dehydrated intermediate. This would suggest that the high activation energy observed for PG transport is related to a high hydrogen bonding capacity of the PG headgroup. In this regard, the activation energy for glycerol transport across EPC bilayers has been variously reported as 11 kcal/mol (Cohen, 1975) or 19 kcal/mol (de Gier et al., 1970). Despite the discrepancy, it would therefore appear that the activation energy observed for PG movement cannot be ascribed solely to the glycerol moiety, indicating that dehydration of the (protonated) phosphate contributes significantly to the observed activation energy.

The influence of the acyl chain length and saturation of the host lipid on PG transport, as well as the influence of cholesterol, is consistent with the influence of these factors on the permeation of small nonelectrolytes across bilayers. For example, increased saturation or chain length of the lipid hydrocarbon decreases the transport of glycerol across bilayers, whereas the inclusion of cholesterol in liquid-crystalline systems markedly reduces the permeability of nonelectrolytes (Bittman & Blau, 1972; Carruthers & Melchior, 1983). Increased saturation, chain length, and the presence of cholesterol all engender increased order and packing of the acyl chain, which is associated with a reduced ability of the permeant species to partition into the hydrocarbon (de Yonge & Dill, 1988).

The remaining point concerns the fact that the induced asymmetry of PG does not approach the inside:outside ratios consistent with transmembrane pH gradients of 2 or more. Three possible explanations for this observation are that the pH gradient is dissipated during the uptake process, that inward transport is inhibited above some critical value due to packing constraints in the inner monolayer, or that the surface charge on the inner monlayer plays an inhibitory role. With regard to possible dissipation of the pH gradient, the pyranine pH reporter indicates that a pH gradient of greater than 2.5 units is maintained for up to an hour during conditions of PG import (EPC/EPG, 9:1; 45 °C) whereas apparent transmembrane equilibrium of PG is achieved by 30 min. The possibility that packing constraints limit the inward or outward transport of PG in response to ΔpH is suggested by the lack of any obvious reverse flow of lipid during the PG redistribution as indicated by the constant lyso-PC transmembrane distribution during PG uptake as detailed here. Clearly, at some point, the imbalance in lipid content between inner and outer monolayers must inhibit further movement of PG due to packing constraints. However, such constraints would not appear to be operating at 5 mol % PG, as at 30 mol % PG more PG is transported into the IM than the total amount of PG in the vesicles containing 5 mol % (Table II). Finally, with regard to surface charge effects, the lack of influence of PS content or the presence of divalent cations described under Results would appear to rule out any direct role. The origins of the low values of the induced PG asymmetry are thus currently not understood.

The ΔpH-induced asymmetry of PG and other lipids which are weak acids has clear biological implications. For example, in thylakoid membranes, ΔpH values of up to 4 units (inside acidic) are observed (Pick et al., 1974; Chow & Hope, 1976), suggesting that minority acidic lipids such as PG would preferentially distribute to the outer monolayer of these membranes. It is clearly possible that detection of such asymmetry may depend on the energy state or intact nature of the organelle. Possible relations to the transbilayer asymmetries observed for PE and PS in plasma membranes such as the erythrocyte are more obscure, as these lipids appear to undergo net movement from the OM to IM via protein-mediated transport (Morrot et al., 1989; Connor & Schroit, 1987). However, it is clear from the results presented here that factors leading to a neutralization of acidic and basic functions in the headgroup of phospholipids may be expected to lead to relatively rapid transmembrane movements.

In summary, the results of this investigation strongly indicate that transmembrane transport of PG in response to pH gradients proceeds via permeation of the uncharged form, possibly as a dehydrated intermediate. The resulting transmembrane redistributions of PG can be extremely rapid, due to the rapid permeation rate of the neutral form which can result in half-times for redistribution on the order of seconds.

REFERENCES

Bishop, W. R. & Bell, R. M. (1985) *Cell 42*, 51–60.
Bittman, R., & Blau, L (1972) *Biochemistry 2*, 4831–4839.
Bretscher, M. S. (1973) *Science 181*, 622–629.
Carruthers, A., & Melchior, D. L. (1983) *Biochemistry 22*, 5797–5807.
Chow, W. S., & Hope, A. B. (1976) *Aust. J. Plant Physiol. 3*, 141–152.
Clement, N. R., & Gould, J. M. (1981) *Biochemistry, 20*, 1534–1538.
Cohen, B. E. (1975) *J. Membr. Biol. 20*, 205–234.
Connor, J., & Schroit, A. J. (1987) *Biochemistry 26*, 5099–5105.
Davis, J. H. (1986) *Chem. Phys. Lipids 40*, 227–258.
Dawidowicz, E. A. (1987) *Curr. Top. Membr. Transp. 29*, 175–202.
de Gier, J., Mandersloot, J. G., Hupkes, J. V., McElhaney, R. N., & van Beek, W. P. (1970) *Biochim. Biophys. Acta 233*, 610–618.
Devaux, P. F., & Seigneuret, M. (1985) *Biochim. Biophys. Acta 822*, 63–125.
de Yonge, L. R., & Dill, K. A. (1988) *Biochemistry, 27*, 5281–5289.
Ganong, B. R., & Bell, R. M. (1984) *Biochemistry 23*, 4977–4983.
Gutnecht, J., & Walter, A (1981a) *Biochim. Biophys. Acta 641*, 183–188.
Gutnecht, J., & Walter, A. (1981b) *Biochim. Biophys. Acta 649*, 149–154.
Higgins, J. A., & Piggot, C. A. (1982) *Biochim. Biophys. Acta 693*, 151–158.
Homan, R., & Pownall, H. J. (1988) *Biochim. Biophys. Acta 938*, 155–166.
Hope, M. J., & Cullis, P. R. (1987) *J. Biol. Chem. 262*, 4360–4366.
Hope, M. J., Bally, M. B., Webb, G., & Cullis, P. R. (1985) *Biochim. Biophys. Acta 812*, 55–65.
Hope, M. J., Redelmeier, T. E., Wong, K. F., Rodrigueza, W., & Cullis, P. R. (1989) *Biochemistry 28*, 4181–4187.
Lange Handbook of Chemistry (1979) (Dean, J. A., Ed.) pp 5.40–5.42, McGraw-Hill Book Co., Toronto.

Lentz, B. R., Madden, S., & Alford, D. R. (1982) *Biochemistry 21*, 6799–6807.

Krebs, J. J. R., Hauser, H., & Carafoli, E. (1979) *J. Biol. Chem. 254*, 5308–5316.

Mandersloot, J. G., Reman, F. C., van Deenen, L. L. M., & de Gier, J. (1975) *Biochim. Biophys. Acta 382*, 22–26.

Mayer, L. D., Hope, M. J., Cullis, P. R., & Janoff, A. S. (1985) *Biochim. Biophys. Acta 817*, 193–196.

McElhaney, R. N. (1986) *Biochem. Cell Biol. 64*, 58–65.

McLaughlin, S. (1975) in *Molecular Mechanisms of Anaesthesia* (Fink, B., Ed.) Vol. 1, pp 193–221, Raven Press, New York.

Morrot, G., Herve, P., Zachowski, A., Fellmann, P., & Devaux, P. F. (1989) *Biochemistry 28*, 3456–3462.

Nash, T. (1953) *Biochem. J. 55*, 416–421.

Nichols, J. W., & Pagano, R. E. (1981) *Biochemistry 20*, 2783–2789.

Op den Kamp, J. A. F. (1979) *Annu. Rev. Biochem. 48*, 47–71.

Pick, U., Rohenberg, H., & Avron, M. (1974) *FEBS Lett. 48*, 32–36.

Seigneuret, M., & Devaux, P. F. (1984) *Proc. Natl. Acad. Sci. U.S.A. 81*, 3751–3755.

Sleight, R. G., & Pagano, R. E. (1984) *J. Cell Biol. 99*, 742–751.

van Meer, G., & Simons, K. (1987) *J. Cell Biol. 105*, 1623–1635.

Watts, A., Harlos, K., Maschke, W., & Marsh, D. (1978) *Biochim. Biophys. Acta 510*, 63–74.

Winiski, A. P., McLaughlin, A. C., McDaniel, R. V., Eisenberg, M., & McLaughlin, S. (1986) *Biochemistry 25*, 8206–8214.

Zachowski, A., Herrmann, A., Paraf, A., & Devaux, P. F. (1987) *Biochim. Biophys. Acta 897*, 197–200.

Folding of Ribonuclease T₁. 1. Existence of Multiple Unfolded States Created by Proline Isomerization[†]

Thomas Kiefhaber,[‡] Rainer Quaas,[§] Ulrich Hahn,[§] and Franz X. Schmid*[‡]

Laboratorium für Biochemie, Universität Bayreuth, D-8580 Bayreuth, West Germany, and Institut für Kristallographie, Abteilung Saenger, Fachbereich Chemie, Freie Universität Berlin, Takustrasse 6, D-1000 Berlin 33, West Germany

Received August 11, 1989; Revised Manuscript Received October 25, 1989

ABSTRACT: It is our aim to elucidate molecular aspects of the mechanism of protein folding. We use ribonuclease T₁ as a model protein, because it is a small single-domain protein with a well-defined secondary and tertiary structure, which is stable in the presence and absence of disulfide bonds. Also, an efficient mutagenesis system is available to produce protein molecules with defined sequence variations. Here we present a preliminary characterization of the folding kinetics of ribonuclease T₁. Its unfolding and refolding reactions are reversible, which is shown by the quantitative recovery of the catalytic activity after an unfolding/refolding cycle. Refolding is a complex process, where native protein is formed on three distinguishable pathways. There are 3.5% fast-folding molecules, which refold within the millisecond time range, and 96.5% slow-folding species, which regain the native state in the time range of minutes to hours. These slow-folding molecules give rise to two major, parallel refolding reactions. The mixture of fast- and slow-folding molecules is produced slowly after unfolding by chain equilibration reactions that show properties of proline isomerization. We conclude that part of the kinetic complexity of RNase T₁ folding can be explained on the basis of the proline model for protein folding. This is supported by the finding that the slow refolding reactions of this protein are accelerated in the presence of the enzyme prolyl isomerase. However, several properties of ribonuclease T₁ refolding, such as the dependence of the relative amplitudes on the probes, used to follow folding, are not readily explained by a simple proline model.

The elucidation of the molecular mechanism of protein folding from a disordered polypeptide chain to the specific native state remains to be one of the major challenges in biochemistry. The information for the native three-dimensional structure and for the folding pathway to this state is apparently encoded in the amino acid sequence of the protein chain. In order to improve our understanding of protein folding and stability, it will be necessary to combine results from theoretical and statistical studies, from protein structure determinations as well as from experiments on the stability and the folding

kinetics. Studies of the kinetics of protein folding aim at the characterization of rate-limiting events on the folding pathway, the detection of partially folded intermediate states, and the elucidation of their relevance for the folding mechanism. Other aspects of the protein folding problem are the role of individual segments of the polypeptide chain for the folding pathway and the formation of secondary structural elements early in folding. Experimental evidence obtained for several small proteins points to an ordered folding mechanism, where secondary structure can indeed be formed rapidly at an early stage. This is followed by slow steps in which ultimately the compact native state is reached (Kim & Baldwin, 1982; Jaenicke, 1987). Similar to the stability of the native protein, the folding mechanism may depend strongly on the solvent conditions chosen for folding. For some proteins, isomerizations of incorrect X–Pro peptide bonds were suggested as rate-limiting